J. Phys. B: At. Mol. Opt. Phys. **31** (1998) 5149–5160. Printed in the UK PII: S0953-4075(98)94419-4

Absolute triple differential cross sections for photo-double ionization of helium—experiment and theory

H Bräuning†‡, R Dörner§, C L Cocke†, M H Prior‡, B Krässig‖, A S Kheifets*, I Bray+, A Bräuning-Demian§, K Carnes†, S Dreuil‡, V Mergel§, P Richard†, J Ullrich¶ and H Schmidt-Böcking§

† Department of Physics, Kansas State University, Manhattan, KA 66506, USA
‡ Lawrence Berkeley National Laboratory, Berkeley, CA 94720, USA
§ Institut für Kernphysik, Universität Frankfurt, August-Euler-Straße 6, D60486 Frankfurt, Germany
‖ Argonne National Laboratory, Argonne, IL 60439, USA
¶ Universität Freiburg, 79104 Freiburg, Germany
* Australian National University, Canberra ACT 0200, Australia
+ Flinders University, GPO Box 2100, Adelaide 5001, Australia

Received 21 May 1998, in final form 22 August 1998

Abstract. We have measured absolute triple differential cross sections for photo-double ionization of helium at 20 eV excess. The measurement covers the full ranges of energy sharing and emission angles of the two photoelectrons. We compare our data for selected geometries with the convergent close-coupling (CCC) calculations as well as 2SC calculations by Pont and Shakeshaft and 3C calculations by Maulbetsch and Briggs. In terms of the absolute magnitude and the trend in the shapes of the triple differential cross section for different geometries we find good agreement of the CCC and published 2SC calculations with our measurement, though differences with respect to the observed shape of individual patterns still exist.

1. Introduction

Double ionization of helium by a single photon has been widely studied over the past few years experimentally as well as theoretically. Although it is one of the simplest many-body processes, discrepancies between experiments and theoretical treatments still exist. Only recently have integral measurements and theoretical calculations of the ratio σ^{++}/σ^{+} of double to single ionization converged [1–4]. For the triple differential cross section (TDCS), however, the overall agreement between theory and experiment is not as good. In a previous paper [5] we presented absolute values of the TDCS for various emission geometries, energy sharing and excess energies. Fourth-order Wannier calculations by Feagin [6, 7] fit the shape of the TDCS very well for all energy sharing at 6 eV above threshold. Not surprisingly the agreement with experiment at 20 eV excess energy and unequal energy sharing is not satisfactory as these configurations are far off the Wannier saddle. Furthermore, the Wannier theory does not yield absolute cross sections.

Two other approaches giving absolute values for the TDCS have been at least partially successful in describing measured cross sections. Maulbetsch and Briggs [8–11] represent the final state by a product of three Coulomb continuum wavefunctions (3C method) which take final state correlation into account directly. The dipole matrix element is evaluated

0953-4075/98/235149+12$19.50

directly. This method, however, fails to give reliable absolute values especially close to the threshold [11] and does not reproduce the dependence of the electron angular asymmetry parameter β on the photo-electron energy [12] very well. In another approach by Pont and Shakeshaft [13–15] the final state is represented by a product of two screened Coulomb wavefunctions (2SC method) employing effective charges. The method employed by Pont and Shakeshaft can, in principle, yield exact results and reproduces well the dependence of β on the electron energy [12].

In an earlier comparative study Maulbetsch *et al* [11] found a good agreement in the relative shapes between the two theoretical methods and experimental data by Schwarzkopf *et al* [16, 17] and Dawber *et al* [18], especially close to threshold or for equal energy sharing. However, in a more recent comparison by Pont *et al* [15] significant differences between the two methods and measurements by Lablanquie *et al* [19] have been found, especially for unequal energy sharing at 4 and 18.6 eV excess energy for the special geometry where one electron is emitted along the polarization axis.

Recently, the convergent close-coupling (CCC) method [20] has been extended to the calculation of photoionization by Kheifets and Bray [21, 22]. The idea is to build on the strength of the CCC method in obtaining accurate electron-impact ionization cross sections [23, 24] by modelling photoionization by a two-step process. The first step has the photon energy totally absorbed by one of the electrons, which then interacts with the residual singly charged ion. Thus, photoionization of helium becomes, to a substantial extent, electron scattering on the He^+ ion. One major difference between photoionization and electron scattering is that the results may be calculated in the three gauges of the electromagnetic operator. It is necessary, though not sufficient, that the results be gauge independent. Yet, this has proved to be particularly difficult in most theoretical approaches. The success of the CCC method for electron–atom scattering suggested that the method is able to accurately obtain the final state. Applying considerable effort towards the description of the initial state, via a 14-term Hylleraas expansion, ensured that the CCC results for photoionization were within a few per cent of each other in all three gauges [22].

Having achieved essentially gauge independence the CCC method was expanded to the calculation of differential $(\gamma, 2e)$ double photoionization [25] along the lines of the CCC method for the calculation of differential $(e, 2e)$ cross sections [26]. Good agreement was found with predominantly relative measurements [25]. Here we study systematically the accuracy of the CCC method by comparison with absolute measurements as the energy sharing of the outgoing electrons is varied from highly asymmetric through to symmetric.

2. Experiment

All measurements presented here were performed at beam-line 7 of the Advanced Light Source at Lawrence Berkeley National Laboratory during double-bunch operation. The photon beam at 99 eV energy was linearly polarized with a Stokes parameter of $S_1 = 0.98 \pm 0.02$. Using the well established technique of cold-target recoil-ion momentum spectroscopy (COLTRIMS) [27] we have measured absolute triple differential cross sections $d^3\sigma/d\Omega_1\, d\Omega_2\, dE_1$ at this energy without any *a priori* restriction to a particular angle or energy for either electron. The experimental set-up and basic data analysis have already been discussed in great detail in [5]. We have extended these measurements by applying a 10 G magnetic field [12] to achieve 4π detection efficiency not only for the recoil ions but also for electrons up to 10 eV in energy. A detailed description of such a novel electron

analyser can be found in [28–31]. From the measured three-dimensional momentum vector of the recoil ion and the detected electron, the full momentum vector of the second electron is calculated using momentum conservation.

The absolute calibration of our data is straightforward. Because at 99 eV photon energy (20 eV excess energy) one electron always fulfils the condition $E_1 \leqslant 10$ eV we have a 4π solid angle detection efficiency for each double-ionization event. Thus the total number of counted electron–He^{2+}-ion coincidences N_0 obtained for the electron energy interval $0 \leqslant E_1 \leqslant 10$ eV corresponds to the total cross section for photo-double ionization σ^{++}. We denote by $N(\theta_1, \theta_2, \phi, E_1)$ the number of events with one electron with energy $E_1 \pm \Delta E/2$ being emitted under a polar angle $\theta_1 \pm \Delta\theta_1/2$ with respect to the polarization axis and the second electron emitted under a polar angle $\theta_2 \pm \Delta\theta_2/2$ with relative azimuthal angle $\phi \pm \Delta\phi/2$ ($\phi = \phi_1 - \phi_2$). The absolute value of the TDCS is then calculated by

$$\frac{\mathrm{d}^3\sigma}{\mathrm{d}E_1\,\mathrm{d}\Omega_1\,\mathrm{d}\Omega_2} = \sigma^{++}\frac{N(\theta_1, \theta_2, \phi, E_1)}{N_0}\frac{1}{2\pi\,\Delta E\,\Delta\phi\int_{\theta_2-\Delta\theta_2/2}^{\theta_2+\Delta\theta_2/2}\sin\theta_2\,\mathrm{d}\theta_2\int_{\theta_1-\Delta\theta_1/2}^{\theta_1+\Delta\theta_1/2}\sin\theta_1\,\mathrm{d}\theta_1}.$$

Here we have integrated over all azimuthal angles ϕ_1 of the first electron, hence the factor 2π. By this integration over ϕ_1 we have implicitly assumed that the differential cross section depends only on the relative azimuthal angle between both electrons and not on the first electron's azimuthal angle relative to the photon beam. This assumption that the very small photon momentum does not break the rotational symmetry around the polarization axis (dipole approximation) is expected to be very well fulfilled at this low photon energy.

The sorting of the data from our spectrometer in constant intervals $\Delta\theta_i$, $\Delta\phi_i$ results in count rates that are proportional to the solid angle element $\Delta\Omega_i = \sin\theta_i\Delta\theta_i\Delta\phi_i$ and therefore the count rate decreases as θ approaches 0° or 180°. In the above equation this effect is accounted for by the factors $\sin\theta_i$ in the denominator. The correction has the negative side effect that any uncertainties resulting from poor statistics in such intervals are dramatically amplified. In the special case of $\theta_1 = 0^\circ$ shown in figure 1(a) we therefore chose the alternative way of sorting the data in constant intervals $\Delta\cos\theta_2$ instead of $\Delta\theta_2$. As a result, the data points for $\theta_1 = 0^\circ$ are not equally spaced in θ_2 and there are no points for $\theta_2 = 0^\circ$ and 180°. This changes the calculation of the TDCS to

$$\frac{\mathrm{d}^3\sigma}{\mathrm{d}E_1\,\mathrm{d}\Omega_1\,\mathrm{d}\Omega_2} = \sigma^{++}\frac{N(\theta_1, \cos\theta_2, E_1)}{N_0}\frac{1}{4\pi^2\Delta E(2/n)\int_0^{\Delta\theta_1}\sin\theta_1\,\mathrm{d}\theta_1}$$

where $N(\theta_1, \cos\theta_2, E_1)$ is the number of electrons with energy 20 eV $- E_1$ emitted in the direction θ_2. n denotes the number of bins in $\cos\theta_2$, i.e. the number of data points in each half-plane of the plots in figure 1(a). To improve our statistics we have made full use of the rotational symmetry of the process with respect to the polarization axis and integrated over the full range of azimuthal angles ϕ_1, ϕ_2, hence the factor $4\pi^2$ in the above equation†. The rotational symmetry is fulfilled by our data; we observe no systematic dependence of the TDCS on ϕ and all fluctuations are within the error bars of $\pm 25\%$. The error bars shown in the figures represent the statistical errors of the integrated data set. Please note that we represent our data for $\theta_1 = 0^\circ$ only in the upper half-plane, as we integrated over the full range of azimuthal angles.

† Strictly, the rotational symmetry applies only for the case of complete linear polarization and for the first electron being emitted exactly along the polarization axis. Using the method described by Schwarzkopf and Schmidt [17] we verified that the slightly lower degree of linear polarization and the finite angular range $\Delta\theta_1 = 20^\circ$ only alters the shape of the TDCS by an amount that is smaller than the experimental error.

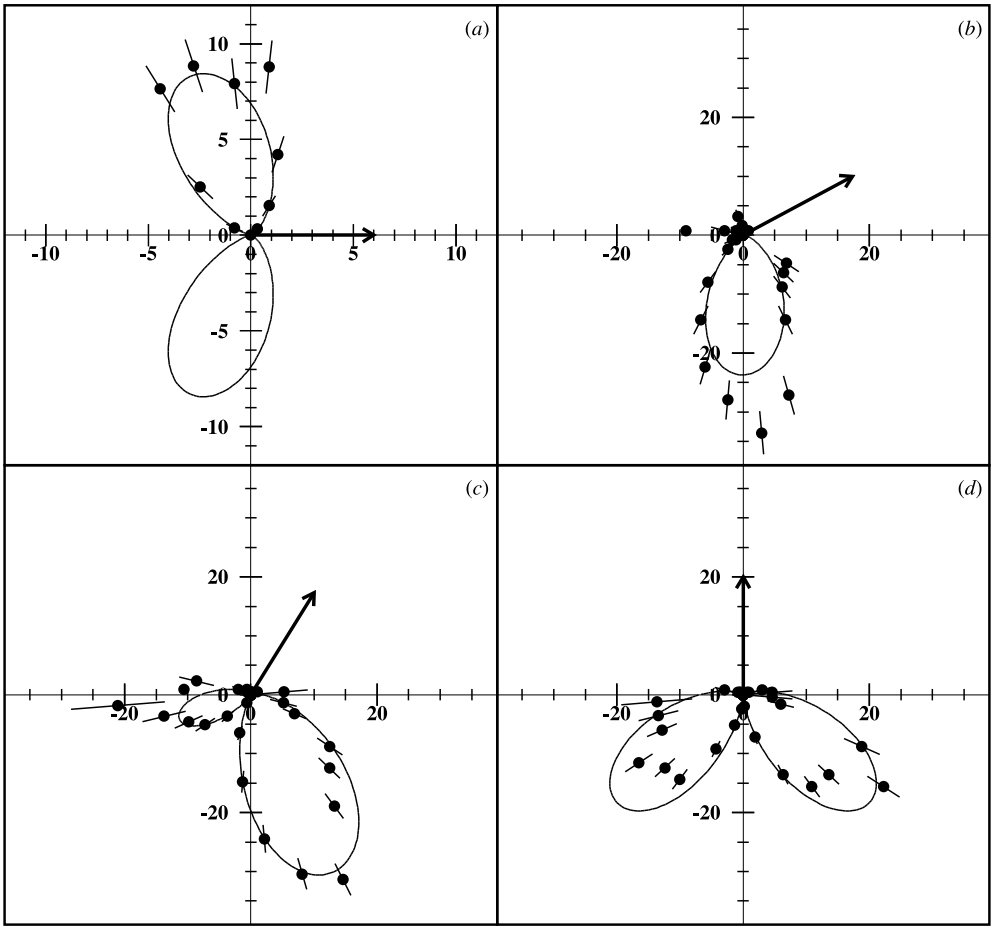

Figure 1. Absolute TDCS in b eV^{-1} sr^{-2} for equal energy sharing and various emissions angles θ_1 of the first electron with respect to the polarization axis: (*a*) $\theta_1 = 0^\circ$, (*b*) $\theta_1 = 30^\circ$, (*c*) $\theta_1 = 60^\circ$ and (*d*) $\theta_1 = 90^\circ$. The curve is the calculated TDCS according to the formulation of Huetz *et al* [37–39] and has been fitted to our data at $\theta_1 = 0^\circ$.

The data have been normalized to the absolute cross section for photo-double ionization of $\sigma^{++} = 8.76$ kb given by Samson *et al* [2]. This value is in excellent agreement with the total cross section $\sigma^+ + \sigma^{++}$ given by Bizeau and Wuilleumier [32] and the ratio of 2.2% of σ^{++}/σ^+ measured by Dörner *et al* [1]. It should be noted that with this normalization procedure the total photon flux, the detection efficiency of the detectors, the gas pressure of the He target, the instrumental resolution and data acquisition dead times do not affect the calibration. The only uncertainties result from the total cross section and the accuracy of the energy and angular gates used for the electron, which is held fixed for generating the TDCS. We estimate the error on the absolute scale to be smaller than 20%.

3. Convergent close-coupling theory

The CCC theory has already been applied to the calculation of double-photoionization TDCS of helium [25]. Presently the treatment of the ground state has been further improved by

the use of a 20-term Hylleraas expansion [33]. This recovers 99.98% of the correlation energy, and leads to excellent agreement between photoionization calculations in the three gauges.

In the present case we calculate photo-double ionization of helium at 99 eV by using a different set of square-integrable expansion states of the final wavefunction, depending on the energy sharing of the outgoing electrons in the experiment. In each calculation, one of the states, for each target-space orbital angular momentum l, has the required experimental secondary energy. Whereas we could employ an interpolation scheme along the lines of the (e, 2e) calculations so that results were obtained for all secondary energies at once [26], we do not do so for photoionization since the calculations are much faster here and we do not wish to compromise any accuracy by invoking interpolation. In all cases we take $l \leqslant 4$, and use approximately $17 - l$ states within each l. The latter is varied so that there was no other state too close to the total energy of 20 eV, thereby avoiding pseudoresonance problems.

A particular peculiarity of the CCC approach to electron-impact ionization, that directly translates to photo-double ionization calculations, is the occurrence of an incoherent combination of amplitudes and the lack of convergence in the singly differential cross section (SDCS), though the integral of the SDCS is convergent. These issues have already been discussed in some detail [34]. Briefly, the CCC method is unable to directly obtain accurate magnitudes whenever the cross section at equal energy sharing is sufficiently large. If this happens, correct results may still be obtained if the shape of the true SDCS is known. The CCC cross sections are rescaled to the true SDCS, obtained by normalizing the true SDCS shape to the CCC integral of the SDCS. In the present case, the true SDCS is found to be relatively flat, which is consistent with the measurements of Wehlitz *et al* [35] and calculations of Pont and Shakeshaft [36]. The CCC total photo-double ionization cross section of helium at 99 eV and its ratio to the single-photoionization cross section are 9.3 ± 0.2 kb and $2.25\% \pm 0.05$, respectively. The variation comes from examining convergence using different basis sizes, which is, though small, larger than the variation in the results of the three gauges within each calculation. Accordingly, the directly calculated CCC SDCS have been rescaled by the factors 1.3, 0.75, 1.0, 1.5 and 2.3 at (1, 19), (3, 17), (5, 15), (7, 13) and (10, 10) eV secondary energies, respectively, to yield SDCS $= 0.93$ kb eV^{-1} for all cases.

4. Results and discussion

Figures 1–5 show our data for 20 eV excess energy on an absolute scale. All figures, except for $\theta_1 = 0^\circ$ are for a coplanar geometry where the polarization axis is horizontal and both electrons are emitted in the plane of the paper. Apart from figure 2, the following acceptance ranges have been used in sorting the data: $\Delta E = 2$ eV for unequal energy sharing, $\Delta E = 4$ eV for equal energy sharing, $\Delta\theta_1 = 20^\circ$ and $\Delta\phi = 20^\circ$. $\Delta\theta_2$ is given by the angular distance of the points in the figures.

It should be noted that the intervals $\Delta\theta_1$, $\Delta\theta_2$, etc are arbitrarily chosen sorting intervals for our event mode data. They are unrelated to the respective instrumental resolutions. The resolution with which the double-ionization events are sorted into such intervals depends very much on their particular geometry. The intrinsic angular resolution in θ_i is about 6° for $\theta_i = 90^\circ$ and deteriorates toward $\theta_i = 0^\circ$ or 180°, where it can be as bad as 20°.

Figure 1 shows the absolute TDCS in b eV^{-1} sr^{-2} for equal energy sharing and various emission angles θ_1. Following the formulation of Huetz and co-workers [37–39] we fitted

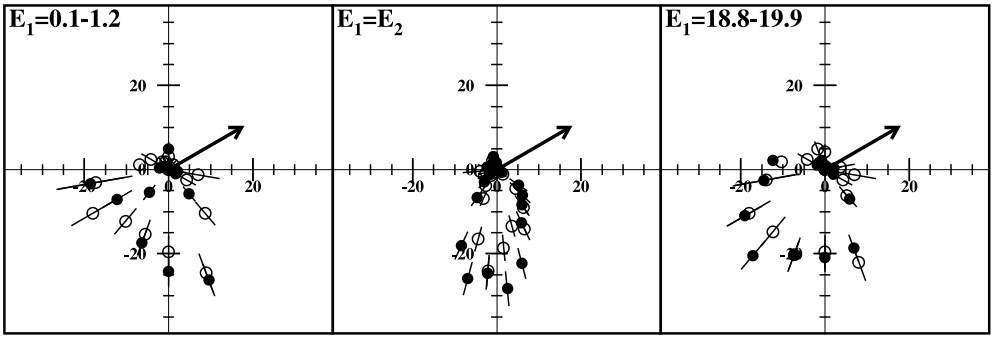

Figure 2. Absolute TDCS in b eV^{-1} sr^{-2} for the coplanar geometry with $\theta_1 = 30^\circ$ and various energy sharing, comparing the data presented in this paper with unrelated previous COLTRIMS measurements. Please note that in this figure we integrated over an azimuthal acceptance angle of $\Delta\phi = 40^\circ$ as it was done in [5] which is twice the value used for other figures as noted in the text. Full circles, this data; open circles, previous COLTRIMS measurement [5].

our data for equal energy in figure 1 with

$$\left.\frac{\mathrm{d}^3\sigma}{\mathrm{d}E_1\,\mathrm{d}\Omega_1\,\mathrm{d}\Omega_2}\right|_{E_1=E_2} = a(\cos\theta_1 + \cos\theta_2)^2 \exp\{-\tfrac{1}{2}[(\theta_{12} - 180^\circ)/\gamma]^2\}$$

where θ_{12} is the angle between the two electrons. From the fit we obtain a full width at half maximum of the Gaussian of $90.2 \pm 2^\circ$. This is in very good agreement with the value of $91 \pm 2^\circ$ by Schwarzkopf and Schmidt [17], $91.6 \pm 2^\circ$ by Dörner *et al* at 20 eV [5] and $91 \pm 2^\circ$ by Malegat *et al* at 18.6 eV excess energy [39]. For the normalization factor a we find a value of $a = 107 \pm 16$ b eV^{-1} sr^{-2}. This is about a factor of 2 larger than the value cited by Schwarzkopf and Schmidt [17], who were the first to perform an absolute measurement of the TDCS using coincident electron spectroscopy and relying only on the known total cross section for single ionization σ^+. However, in a later communication [40] they pointed out that integrating their measured TDCS underestimates the total cross section σ^{++} by a factor of about 2.

Figure 2 compares our recent data with data published in [5] from a previous experiment†, where no 4π detection efficiency had been achieved due to the lack of a magnetic field. The good agreement between these two sets of data which have been analysed and normalized completely independently of each other show the very good reproducibility of our experimental procedure.

Figure 3 shows the dependence of the TDCS on θ_1 and the energy sharing. For $\theta_1 = 90^\circ$ (right-hand column) the $^1S^e$ symmetry of the initial state, the corresponding $^1P^o$ symmetry of the final state and the linear polarization of the light result in a vanishing TDCS for $\theta_2 = 90^\circ$ regardless of energy sharing [8]. For equal energy sharing (top row) back-to-back emission is forbidden due to the positive parity of the initial state and the required negative parity of the final state (as the electron pair has total spin zero, a state where both electrons are emitted back-to-back has positive parity). Both selection rules are clearly shown by our data and no energy dependence of the TDCS is observed for $\theta_1 = 90^\circ$. For $\theta_1 = 60^\circ$ (middle column) back-to-back emission is still suppressed for unequal energy

† In our previous paper [5] the figures for unequal energy sharing concerning $E_\gamma = 99$ eV are mislabelled. Figure 14 lower row left-hand panel and figure 15 left-hand column upper panel should read $E_1/E = 0$–0.05 (instead of 0–0.2); figure 14 lower row right-hand panel and figure 15 left-hand column lower panel should read $E_1/E = 0.95$–1 (instead of 0.8–1).

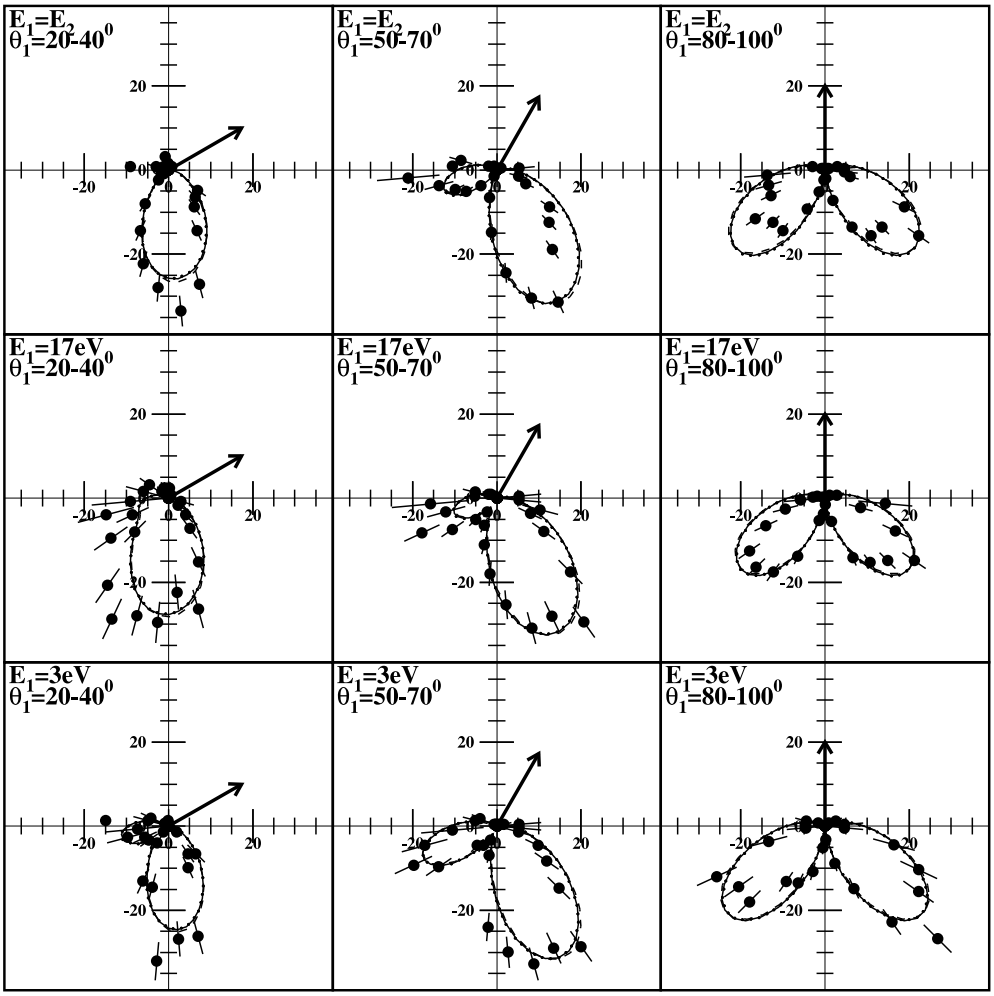

Figure 3. Absolute TDCS in b eV^{-1} sr^{-2} in comparison with CCC calculations. The various gauges used for the calculations are plotted, but in most cases cannot be distinguished: full curve, velocity form; broken curve, length form; dotted curve, acceleration form.

sharing and no significant dependence of the TDCS on the energy sharing can be seen. Only for $\theta_1 = 30^\circ$ (left-hand column) do we find significant changes in the form of the TDCS between equal and unequal energy sharing. In particular, for $E_1 = 17$ eV the node for back-to-back emission of the two electrons vanishes completely. The shape as well as the absolute value of the experimental TDCS is very well reproduced by the CCC calculations, which are shown by full, broken and dotted curves representing the velocity, length and acceleration gauge, respectively. The slight differences in absolute height in some plots between experiment and theory are within the error of our absolute normalization. The dependence of the TDCS on the energy sharing is shown in more detail in figure 4 for fixed $\theta_1 = 30^\circ$. No significant change in the form of the TDCS is observed over a wide range of different energy sharing. For extremely unequal energy sharing (i.e. $E_1 = 1$ or 19 eV) the form of the TDCS changes and back-to-back emission of the electrons becomes enhanced

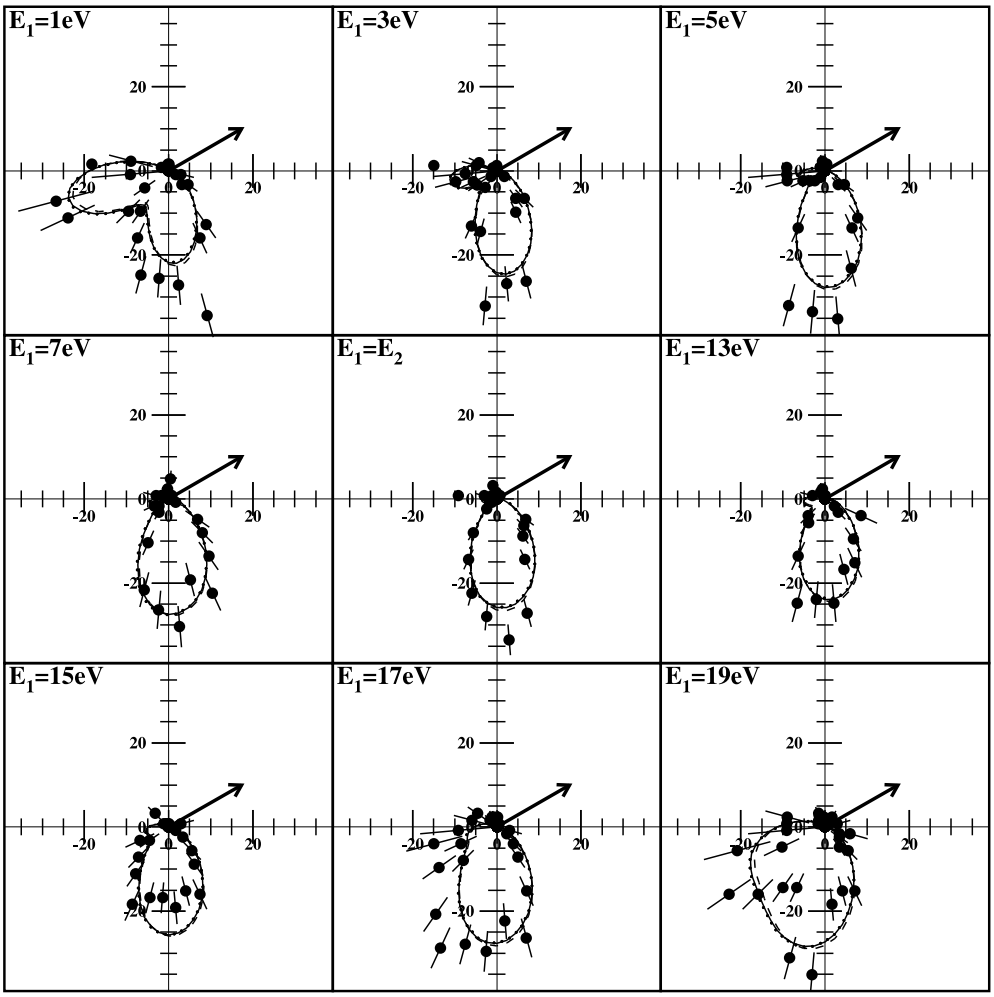

Figure 4. Absolute TDCS in b eV^{-1} sr^{-2} for $\theta_1 = 30^\circ$ as a function of the energy sharing. The curves are CCC calculations in velocity form (full), length form (broken) and acceleration form (dotted).

(see also figure 2). Furthermore, while for very small E_1/E the TDCS shows a two-lobed structure only one single lobe is observed for very large E_1/E.

Figure 5 shows the TDCS for the special case of $\theta_1 = 0^\circ$ where the effect of energy sharing on the TDCS is most pronounced. Here the TDCS for back-to-back emission becomes a maximum for unequal energy sharing as was first observed by Schwarzkopf and Schmidt [17] and is also clearly shown by our data. Relative measurements by Mazeau *et al* [41] also show this filling of the node at 18.6 eV above threshold. The relative shape of their measured TDCS, however, does not agree well with the theoretical calculations [15] and is also different from the data presented here. Keeping the slow electron fixed our data show a clear lobe perpendicular to the polarization axis (see figures 5(c) and (f)) which is not visible in their data. In the case of the fast electron being fixed the shapes of our measured TDCS and their data appear rather similar, elongated along the polarization axis with the maximum for back-to-back emission.

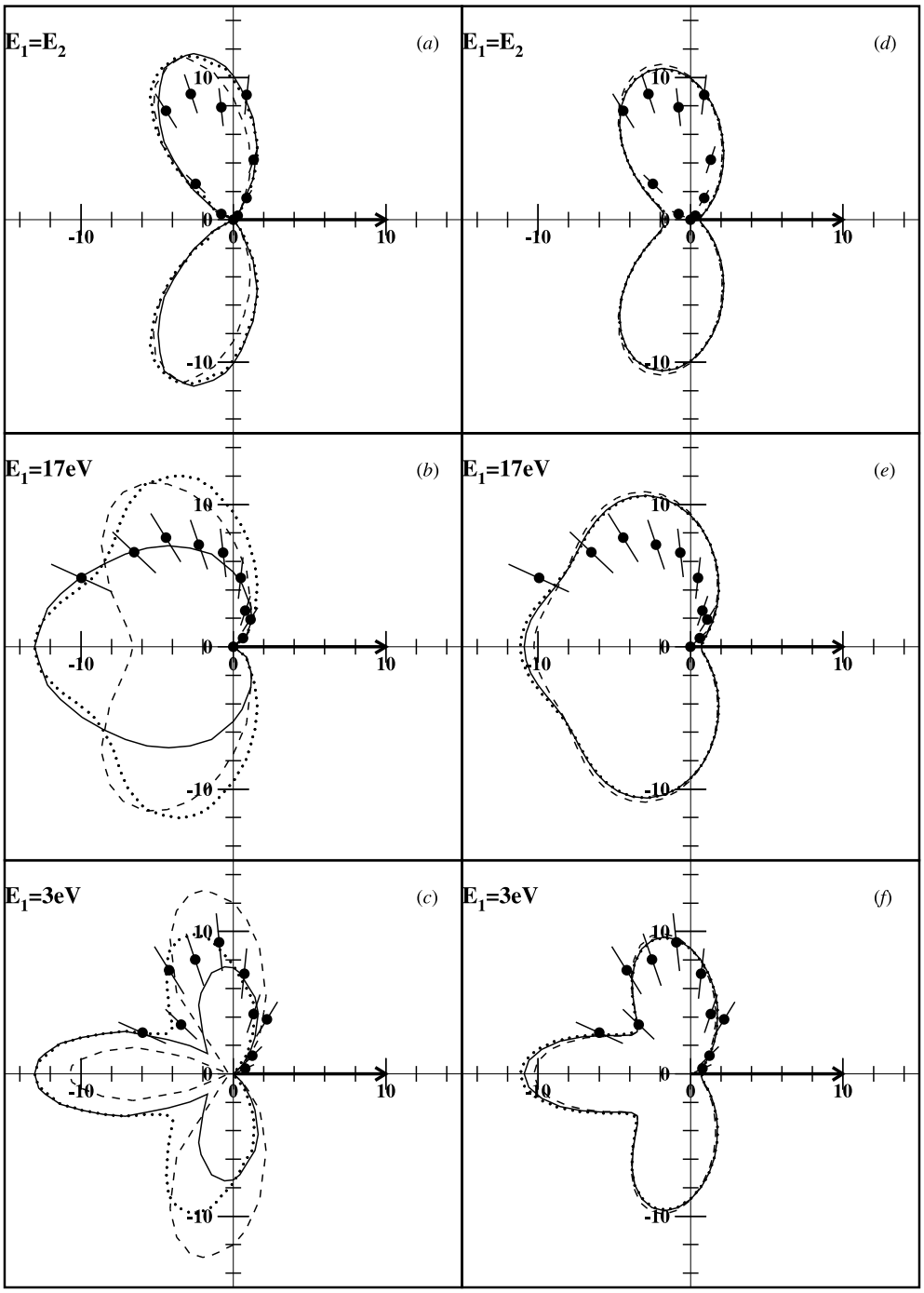

Figure 5. Absolute TDCS in b eV^{-1} sr^{-2} for $\theta_1 = 0^\circ$ and various energy sharing. The curves in (*a*)–(*c*) are 3C calculations in velocity form (full), 3C calculations in length form (broken) and 2SC calculations (dotted) [15]. The curves in (*d*)–(*f*) represent CCC calculations in velocity form (full), length form (broken) and acceleration form (dotted).

The figure compares our data with the CCC calculations (right-hand column), the 2SC calculations in the velocity gauge (left-hand column, dotted curve) and the 3C calculations in the velocity (left-hand column, full curve) and length gauge (left-hand column, broken curve) from [15]. The CCC and 2SC calculations are presented on an absolute scale in units of b eV^{-1} sr^{-2}. The absolute TDCS calculated with the 3C method in the velocity gauge is about a factor 2 higher at 20 eV excess energy than the value given by the 2SC calculations [11]. The 3C calculations have been rescaled by [15] to the same TDCS at its maximum for comparison. Only the CCC calculations have been performed directly for 20 eV excess energy. The 2SC and 3C calculations are taken from [15] and were performed for 18.6 eV excess energy.

For equal energy sharing the 2SC and 3C calculations show good agreement in shape with each other and the experimental data. On an absolute scale we also find good agreement between the 2SC calculation and our data within the error of our absolute normalization. The CCC calculations agree in overall shape with the other calculations and our experimental data and are in very good agreement with the data on an absolute scale. However, they do not reproduce well the node for $\theta_2 = 180^\circ$ in the case of equal energy sharing. This is due to the fact that the electrons are not treated in an identical manner within the CCC framework. The fact that the cross sections do turn out to be small, where they should be zero due to indistinguishability of electrons, is an encouraging confirmation of the CCC approach to the treatment of the two-electron continuum.

For unequal energy sharing there are significant differences in the 2SC and 3C calculations and also within the 3C calculations for the different gauges. The problem of the dependence of the TDCS on the various gauges has been addressed in depth in a recent study by Lucey *et al* [42]. The CCC calculations, which yield the same results independent of the gauge used, show the same overall shape and similar absolute magnitude as the 2SC calculations. The comparison of the theoretical calculations with the experimental data, however, does not give a fully consistent picture. The CCC and 2SC calculations show perfect agreement in shape and absolute magnitude with the experimental data for $E_1 = 3$ eV, but deviate somewhat at $E_1 = 17$ eV. Conversely, the velocity-gauge 3C calculation shows very good agreement in shape at $E_1 = 17$ eV and deviates for $E_1 = 3$ eV, but large discrepancies exist for the other gauges and the absolute magnitude. The theoretical TDCS are generated from calculated matrix elements which are the same for both energies, and should therefore be either correct or wrong in both cases. The assessment of agreement between theory and experiment has thus to be based not only on a single pattern, but on a variety of different geometries, as we have attempted to do for the CCC calculations in figures 3 and 4. In this comparison the results of our CCC calculation successfully reproduce the absolute magnitude and the trend in shapes of the experimental TDCS patterns.

5. Conclusions

The ability of the COLTRIMS technique to detect double-ionization events with 4π collection efficiency and to simultaneously obtain the full kinematic information allowed us to determine TDCS angular patterns at 20 eV excess energy on an absolute scale and for arbitrary geometries. This afforded us the opportunity of a comprehensive comparison of selected experimental TDCS patterns with theoretical descriptions. We present results of CCC calculations, which are essentially gauge independent. These calculations have been rescaled assuming a flat SDCS to give absolute values. In the case of $\theta_1 = 0^\circ$ the theoretical results are in fairly good agreement with the 2SC results of Pont and Shakeshaft

published for 18.6 eV excess energy. In the comparison with the experiment generally good agreement of the CCC calculations with the presented set of experimental TDCS has been found for their absolute magnitudes and, to a somewhat lesser degree, their shapes.

The success of the CCC theory raises the question of just how accurate such calculations are and the method generally. Given that the CCC theory treats the outgoing electrons in a highly asymmetric manner, a further stringent test of the theory would be to reduce the total energy of the system, while still maintaining good experimental statistics.

Acknowledgments

This work was supported by the Division of Chemical Sciences, Office of Basic Energy Sciences, Office of Energy Research, US Department of Energy, the Max Planck Preis of the Alexander von Humboldt-Stiftung, the DFG and BMBF, the Graduiertenförderung des Landes Hessens and the Willkomm Foundation. HB gratefully acknowledges support from the Alexander von Humboldt Foundation and RD from the Habilitandenprogamm of the DFG. We thank R Thatcher, T Warwick, E Rothenberg, J Denlinger and the entire support staff of the ALS for their excellent support. IB acknowledges the support of the Australian Research Council and the South Australian Center for High Performance Computing and Communications.

References

[1] Dörner R *et al* 1996 *Phys. Rev. Lett.* **76** 2654
[2] Samson J A R, Stolte W C, He Z X, Cutler J N, Lu Y and Bartlett R J 1998 *Phys. Rev.* A **57** 1906
[3] Qiu Y, Tang J-Z, Burgdörfer J and Wang J 1998 *Phys. Rev.* A **57** R1489
[4] Kheifets A S and Bray I 1998 *Phys. Rev.* A **57** 2590
[5] Dörner R *et al* 1998 *Phys. Rev.* A **57** 1074
[6] Feagin J M 1995 *J. Phys. B: At. Mol. Opt. Phys.* **28** 1495
[7] Feagin J M 1996 *J. Phys. B: At. Mol. Opt. Phys.* **29** l551
[8] Maulbetsch F and Briggs J S 1993 *J. Phys. B: At. Mol. Opt. Phys.* **26** 1679
[9] Maulbetsch F and Briggs J S 1993 *J. Phys. B: At. Mol. Opt. Phys.* **26** L647
[10] Maulbetsch F and Briggs J S 1994 *J. Phys. B: At. Mol. Opt. Phys.* **27** 4095
[11] Maulbetsch F, Pont M, Briggs J S and Shakeshaft R 1995 *J. Phys. B: At. Mol. Opt. Phys.* **28** L341
[12] Bräuning H *et al* 1997 *J. Phys. B: At. Mol. Opt. Phys.* B **30** L649
[13] Proulx D and Shakeshaft R 1993 *Phys. Rev.* A **48** R875
[14] Pont M and Shakeshaft R 1995 *Phys. Rev.* A **51** R2676
[15] Pont M, Shakeshaft R, Maulbetsch F and Briggs J S 1996 *Phys. Rev.* A **53** 3671
[16] Schwarzkopf O, Krässig B, Elmiger J and Schmidt V 1993 *Phys. Rev. Lett.* **70** 3008
[17] Schwarzkopf O and Schmidt V 1995 *J. Phys. B: At. Mol. Opt. Phys.* **28** 2847
[18] Dawber G, Avaldi L, McConkey A G, Rojas H, MacDonald M A and King G C 1995 *J. Phys. B: At. Mol. Opt. Phys.* **28** L271
[19] Lablanquie P, Mazeau J, Andric L, Selles P and Huetz A 1995 *Phys. Rev. Lett.* **74** 2192
[20] Bray I and Stelbovics A T 1992 *Phys. Rev.* A **46** 6995–7011
[21] Kheifets A and Bray I 1996 *Phys. Rev.* A **54** R995–8
[22] Kheifets A and Bray I 1998 *Phys. Rev.* A **57** 2590–5
[23] Bray I and Stelbovics A T 1993 *Phys. Rev. Lett.* **70** 746–9
[24] Bray I, McCarthy I E, Wigley J and Stelbovics A T 1993 *J. Phys. B: At. Mol. Opt. Phys.* **26** L831–6
[25] Kheifets A and Bray I 1998 *J. Phys. B: At. Mol. Opt. Phys.* **31** L447–53
[26] Bray I and Fursa D V 1996 *Phys. Rev.* A **54** 2991–3004
[27] Ullrich J, Moshammer R, Dörner R, Jagutzki O, Mergel V, Schmidt-Böcking H and Spielberger L 1997 *J. Phys. B: At. Mol. Opt. Phys.* **30** 2917
[28] Moshammer R *et al* 1994 *Phys. Rev. Lett.* **73** 3371
[29] Moshammer R, Ullrich J, Unverzagt M, Schmitt W, Jardin P, Olson R E, Dörner R, Mergel V and Schmidt-Böcking H 1996 *Nucl. Instrum. Methods* B **107** 62

[30] Moshammer R, Unverzagt M, Schmitt W, Ullrich J and Schmidt-Böcking H 1996 *Nucl. Instrum. Methods* B **108** 425
[31] Ullrich J, Moshammer R, Unverzagt M, Schmidt W, Jardin P, Olson R E, Dörner R, Mergel V and Schmidt-Böcking H 1995 *Nucl. Instrum. Methods* B **98** 375
[32] Bizeau J M and Wuilleumier F 1995 *J. Electron Spectrosc. Related Phenom.* **71** 205
[33] Hart J F and Herzberg G 1957 Twenty-parameter eigenfunctions and energy values of the ground states of He and He-like ions. *Phys. Rev.* **106** 79–82
[34] Bray I 1997 *Phys. Rev. Lett.* **78** 4721–4
[35] Wehlitz R, Heiser F, Hemmers O, Langer B, Menzel A and Becker U 1991 *Phys. Rev. Lett.* **67** 3764–7
[36] Pont M and Shakeshaft R 1995 *J. Phys. B: At. Mol. Opt. Phys.* **28** L571–7
[37] Huetz A, Selles P, Waymel P and Mazeau J 1991 *J. Phys. B: At. Mol. Opt. Phys.* **24** 1917
[38] Malegat L, Selles P and Huetz A 1997 *J. Phys. B: At. Mol. Opt. Phys.* **30** 251
[39] Malegat L, Selles P, Lablanquie P, Mazeau J and Huetz A 1997 *J. Phys. B: At. Mol. Opt. Phys.* **30** 263
[40] Schwarzkopf O and Schmidt V 1996 *J. Phys. B: At. Mol. Opt. Phys.* **29** 1877
[41] Mazeau J, Andric L, Jean A, Lablanquie P, Selles P and Huetz A 1996 *Atomic and Molecular Photoionization* ed A Yagishita and T Sazaki, Tokyo p 31
[42] Lucey S P, Rasch J, Whelan C T and Walters H R J 1998 *J. Phys. B: At. Mol. Opt. Phys.* **31** 1237